INVESTIGATION OF ATTENUATION BEHAVIOUR AND WAVE PROPAGATION OF GAS INSULATED TRANSMISSION LINES (GIL)

F. Goll[1*], R. Witzmann[1], U. Schichler[2], C. Neumann[3]
[1]Technische Universität München, Arcisstraße 21, 80290 München, Germany
[2]SIEMENS AG, E T HS MF TS, Nonnendammallee 104, 13629 Berlin, Germany
[3]Amprion GmbH, Rheinlanddamm 24, 44139 Dortmund, Germany
*Email: <felix.goll@tum.de>

Abstract: Measurements on a 400 kV GIL with a length of approximately 900 m have been performed in Kelsterbach near Frankfurt, Germany. Travelling waves have been generated by operation of an earthing switch and measured at different locations along the Gas Insulated Transmission Line (GIL). The propagation velocity of the travelling waves in the GIL has been investigated by analysing the steep front signals at different measuring locations. By means of different terminations and setups allowing or avoiding outcoupling of travelling waves onto the external feed-in system, the internal damping of such a transmission system has been investigated. The resistive and inductive behaviour of the burning arc in the switching gap of the earting switch was taken into account. The results have been compared to theoretical calculations which are based on the frequency dependent line parameters of the GIL. The advantage of the availability of different measuring points at such long transmission systems for the detection of an internal flashover is explained.

1 INTRODUCTION

The proportion of renewable energy systems on the electrical power generation is increasing continuously in line with the political and social aims. Especially the upcoming offshore wind parks in the North Sea are expected to have a major impact on the future power system in Germany. New transmission capacity is needed, especially in the extra high voltage range, to integrate the renewable power into the present energy system.

Building new high voltage overhead lines is becoming more and more difficult due to the approval processes and the limited public acceptance. Therefore underground transmission line solutions also for hybrid transmission systems have to be developed. Research activity on gas insulated transmission lines as an alternative to conventional high voltage cables has recently been increased. Those GIL systems have advantages compared to conventional cables in thermal transmission capacity and operational aspects.

To investigate the transient behaviour of long hybrid transmission systems consisting of overhead lines as well as GIL sections especially concerning insulation coordination simulation models viable up to the MHz range are necessary.

2 MEASUREMENTS

2.1 Test setup

Two parallel 400 kV GIL systems with a transmission length of approximately 900 m are installed near Frankfurt, Germany (see Figure 1) [1].

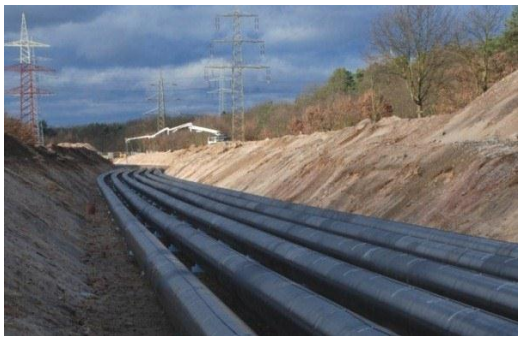

Figure 1: Trench with GIL phases

The GIL systems are terminated at one end by a gas insulated substation (GIS) and on the other end by the bushings connecting the overhead lines (feed-in). The test voltage is generated by a resonant test circuit and fed into the GIL via the overhead line bushings (Figure 3). Three distributed measuring points (MP-8, MP300, MP800) equipped with VFT-sensors are available and were used for measurements (Figure 2).

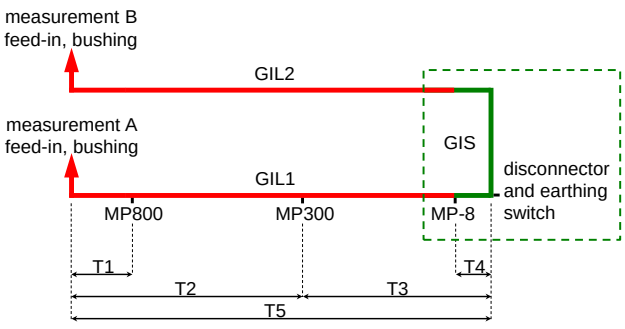

Figure 2: Test setup with three distributed measuring points: MP-8, MP300, MP800. T1-T5 marking travelling times (see Table 1).

Generation of travelling waves

The test system is charged to 150 kV. An earthing switch, see Figure 4, inside the GIS is switched on and causes a pre-arcing, which results in the propagation of travelling waves. A rise time of 12 ns was measured.

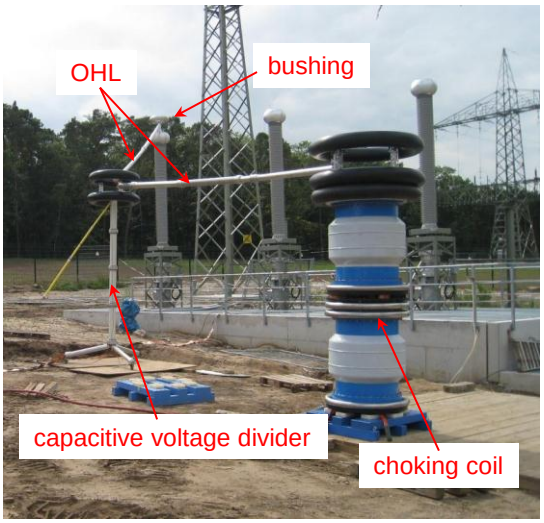

Figure 3: Feed-in and resonant test set.

Two scenarios depending on the location of the feed-in and the switching position of the disconnector were analysed (compare to Figure 2 and Figure 4):

- Measurement A: Feed-in at GIL1; disconnector is in open position. The travelling waves are allowed for outcoupling to the feed-in system.

- Measurement B: Feed-in at GIL2; disconnector is in closed position and the analysed GIL1 is connected to the GIL2 system. The outcoupling of travelling waves at the analysed GIL1 onto the external feed-in system is thus avoided.

For the travelling waves both scenarios are terminated as the follows:

The travelling waves are reflected in the area of the feed-in at an inductivity (choking coil, measurement A) or at the open end of the bushing (measurement B), both resulting in a reflection factor of +1.

On the other end – inside the GIS – the burning arc acts as a short circuit and therefore the travelling waves are reflected with a reflection factor of -1.

2.2 Voltages at measurement points

The resulting voltage waveforms for measurement A observed at the three measuring points are shown in Figure 5. The steep front signals are marked, in which

- digit “1” marks the steep travelling wavefront, generated by the earthing switch,

- digit “2” represents the steep front reflected by the junction between the GIL and OHL (end of the bushing) and

- digit “3” marks the reflection of the travelling waves caused by the burning arc at the earthing switch.

These steep front signals can be observed at every measuring point in a certain time difference corresponding to the relevant geometric distance.

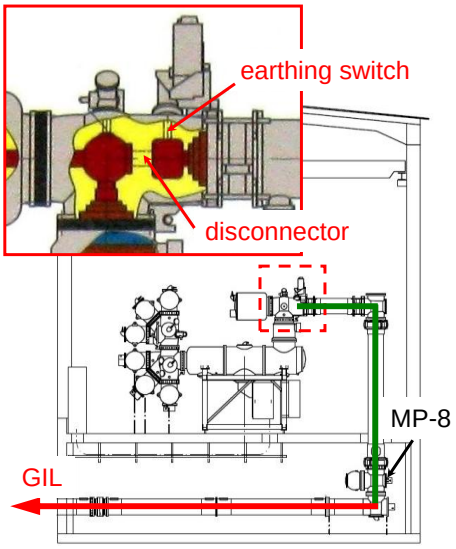

Figure 4: Earthing switch and disconnector within the GIS (compare Figure 2).

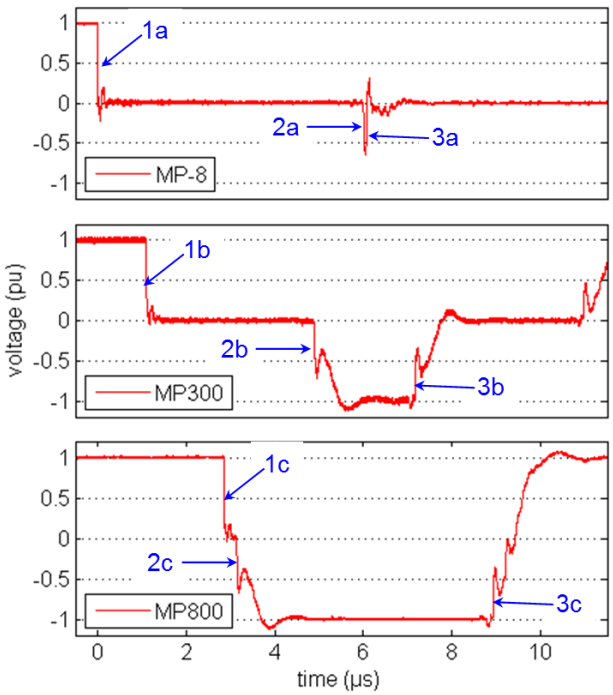

Figure 5: Voltage waveforms at the three measurement points (measurement A).

2.3 Propagation velocity

Using the three different measuring points and the recorded steep fronts the propagation velocity of the travelling waves within the GIL could be determined.

The elapsed time between mark “1b” and “2b” represents twice the travelling time of the signal between measuring points MP300 and the junction between the GIL and OHL (end of the bushing).

This kind of analysis was done for all three measuring points. The resulting time difference is halved and the average of different measurements was taken. Table 1 summarises these results.

From GPS-measurements the system length is known, e.g. the distance between measuring point MP-8 and MP800 is 851.04 m. With the travelling time according to T5-T1-T4 the propagation velocity of the travelling waves can be evaluated to be 99.2 % of the speed of light (300000 km/s). Further calculations confirm this figure. This value is very close to the ideal propagation velocity compared to previous measurements [2].

Table 1: Average travelling times for distances corresponding to Figure 2.

	T1	T2	T3	T4	T5
average time duration in ns	142.2	1899.1	1134.9	32.0	3033.6

2.4 Attenuation

It is possible to measure the signal without significant distortion or reflection after a travelling distance of around 530 m, i.e. the distance between measuring point MP300 and measuring point MP800. Measuring point MP-8 cannot be used for this analysis because it is positioned inside the GIS. That means that the incoming signal is overlaid with the reflected signal due to the change of the characteristic impedance between GIS and GIL.

The measured steep front signals “1b” according to MP300 and “1c” according to MP800 are shown in Figure 6; both measuring points were equipped simultaneously with the identical measuring technique. An attenuation effect of the GIL after the distance of around 530 m cannot be observed. Six disc insulators are installed within this length.

2.5 Long-time measurements

According to the test setup, the travelling waves are reflected at both ends of the GIL with a reflection factor of +1 and -1 respectively. Measurements have been performed until the signal was completely damped. This complete attenuation was also analysed.

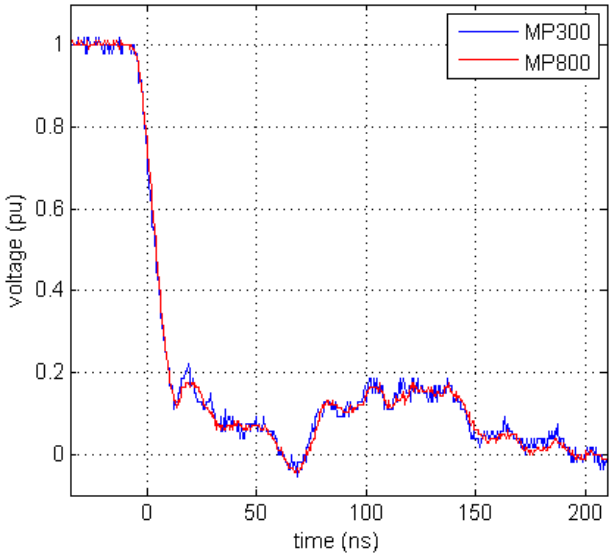

Figure 6: Waveform of the travelling waves after a distance of approximately 530 m.

For both measurement A and B the breakdown voltage was identical, resulting in the same damping conditions caused by the burning arc. The voltage profiles given in Figure 7 indicate, that the damping of the test setup which allows the outcoupling to the feed-in system (measurement A) is higher than the damping with avoided outcoupling (measurement B).

The decay time was chosen to an oscillation amplitude of around 2.5 % of the breakdown voltage. For measurement A this is approx. 1.51 ms and for measurement B approx. 1.85 ms.

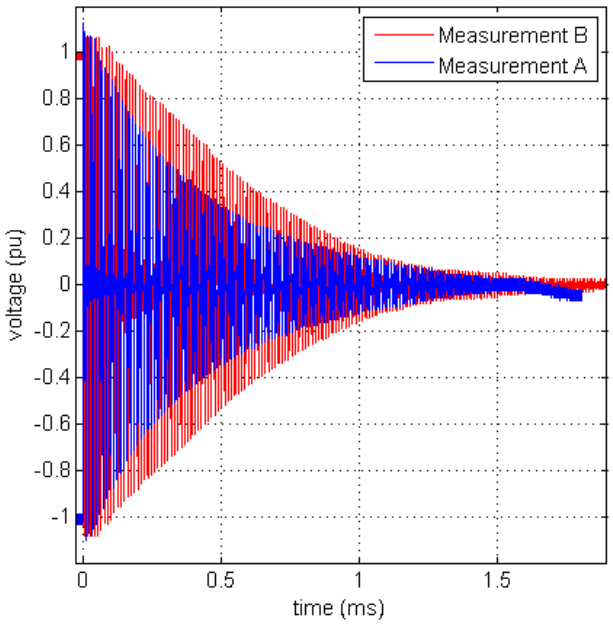

Figure 7: Damping of the travelling waves on the test setup measured at MP300.

An attenuation per period depending on different breakdown voltages according to Table 2 can be derived. Hence, it can be concluded that the outcoupling of the travelling waves onto the feed-in

system causes approximately 25 % of the complete system damping.

Table 2: Measured attenuation per period.

Measurement A	Measurement B
2.4 % - 3.0 %	1.75 % - 2.7 %

3 TIME DOMAIN ATTENUATION

The complete damping behaviour according to the long-time measurements in chapter 2.5 was simulated. The dynamic network calculation program NETOMAC was used and the scenario acc. measurement A is modelled. The OHL, GIL and GIS devices of the experimental setup are modelled without losses according to the Bergeron model.

The complete test setup includes three attenuation effects for the travelling waves:

- Attenuation caused by outcoupling to the feed-in and earthing system,
- attenuation caused by the burning arc and
- attenuation caused by the gas insulated transmission line, including several disc insulators.

The attenuation influence due to outcoupling of the travelling waves (e.g. radiation, resistance of the earthing system) is estimated to be 25 % of the complete system damping (according to Table 2) and is not explicitly modelled.

Thus, the only damping effect included in the time domain simulations is the influence of the burning arc. This physical effect is modelled according to Figure 8 [3].

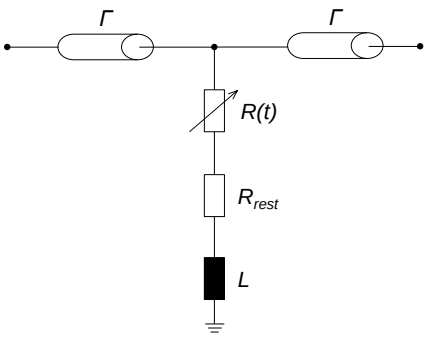

Figure 8: Model of the burning arc caused by the earthing switch.

The voltage breakdown due to the flashover is simulated by a variable resistance *R(t)* due to Toepler's law [4].

$$R(t) = \frac{k_T \cdot l}{\int_0^t i \cdot dt} \quad (1)$$

where $R(t)$ = time dependent resistance (Ω)
k_T = Toepler's constant ($2.4 \cdot 10^{-4}$ Vs/cm)
l = length of burning arc (0.8 cm)
i = current through burning arc (A)

For the very high frequencies the inductance can be calculated by Equation 2 according to [5].

$$L = \mu_0 \cdot \frac{l}{2\pi} \cdot \left(\ln \frac{2l}{r} - 1 \right) \quad (2)$$

where L = inductivity of arc/conductor (H)
μ_0 = magnetic constant ($4 \cdot \pi \cdot 10^{-7}$ Vs/Am)
l = length of arc/conductor (m)
r = radius of arc/conductor (m)

The complete inductivity L is made up of the inductivity of the burning arc and the inductivity of the contact pin of the earthing switch. Different radii and lengths of the arc and the earthing switch are taken into account. The differences are marginal, so that for the simulations a constant inductivity of 38.5 nH was assumed.

The damping influence of the burning arc is due to the residual resistance R_{rest}. For simulations with R_{rest} of 0.35 Ω and 0.45 Ω the signal is damped to around 2,5 % after 2.29 ms and 1.76 ms respectively.

Taking the attenuation of 25 % due to outcoupling into account the simulated signal would be damped after 1.72 ms and 1.32 ms respectively. The measured value of 1.51 ms is between these two simulated values.

In [3] a similar setup with a flashover caused by a locked earthing switch is measured under laboratory conditions. The main difference is the higher breakdown voltage of 370 kV, what results in a higher distance of 2 cm between earthing switch and inner conducter. The best accordance between measurement and simulation were obtained in this laboratory study with a constant residual resistance R_{rest} of 0.5 Ω.

The distance between the earthing switch and the inner conductor at a breakdown voltage of around 150 kV according to the measurements on the real GIL can be estimated to be around 0.8 cm. Therefore the residual resistance has to be lower than 0.5 Ω.

Hence the assumed values for R_{rest} of 0.35 Ω and 0.45 Ω respectively are in a reasonable range.

Both attenuation effects due to the termination of the GIL – outcoupling to the external system and

spark resistance – are taken into account for the time domain simulations and the simulated decay time is in the range of the measured time. Thus, it is not possible to identify the internal attenuation influence of the gas insulated transmission line with the included disc insulators itself.

4 FREQUENCY DOMAIN CALCULATIONS

In order to quantify the internal damping of the GIL a software tool which takes the frequency depending line parameters of the GIL into account was written to calculate the signal transformation due to the transmission characteristic of the line.

An arbitrary voltage u_1 is distorted and damped by a transmission line after a certain distance x to the voltage signal u_2 according to Equation 3 [6].

$$u_2 = u_1 \cdot e^{-(\alpha+\beta)\cdot x} = u_1 \cdot e^{-\gamma \cdot x} \qquad (3)$$

where u_1 = incoming voltage (pu)
u_2 = outgoing voltage after distance x (pu)
γ = propagation constant (1/m)
α = attenuation constant (1/m)
β = phase constant (1/m)
x = line length (m)

The attenuation constant α as well as the phase constant β are both increasing with increasing frequency and are resulting from the frequency dependent line parameters resistance R', shunt conductance G', capacitance C' and inductance L'.

The damping of the disc insulators is disregarded in these frequency domain calculations.

The software tool transforms an arbitrary signal given in the time domain into the frequency domain by the use of the Fourier transformation. In the frequency domain, every frequency component is modulated with its corresponding propagation constant $\gamma(f)$ and a certain line length x. Afterwards, this modified frequency spectrum is transformed back into the time domain by the Inverse Fourier Transformation as shown in Figure 9.

For a qualitative verification of this software tool the measured signal “1b” at measuring point MP300 was used and the attenuation after 530 m, i.e. the distance to measuring point MP800 was computed.

Similar to the measurement acc. to Figure 6 no attenuation after a distance of 530 m is obtained, so the calculation tool gives a reasonable result.

For insulation coordination studies, the damping of a lightning impulse voltage is more interesting. The result according to the frequency domain modulation through a gas insulated transmission line with a length of 25 km is given in Figure 10. Only a slight damping is obtained; the peak value is attenuated to 98.7 % and the signal shape is nearly unaffected. Simulation with a length of 2 km did not show a difference between incoming and outgoing signal.

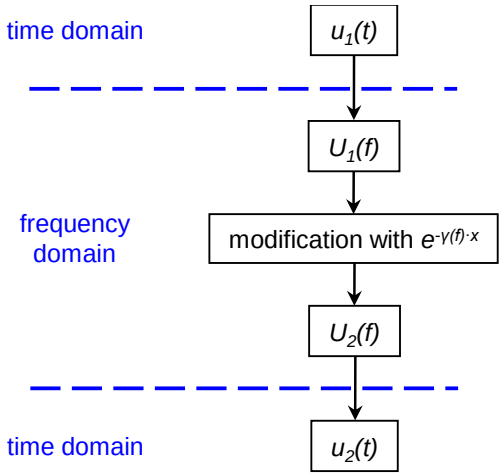

Figure 9: Main principle of frequency domain calculations.

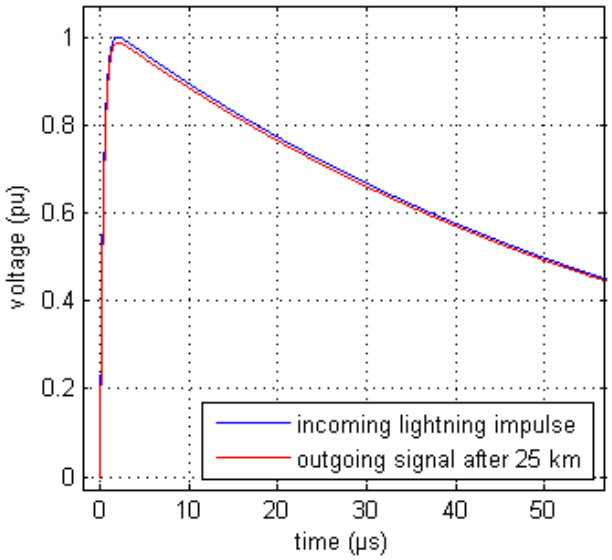

Figure 10: Attenuation after 25 km of a lightning impulse signal.

This calculation shows that the GIL has nearly no attenuation influence on lightning impulse voltages for a transmission distance of some kilometers.

5 DETECTION OF INTERNAL FLASHOVER

For the detection of the location of an internal fault in a long GIL, VFT–measuring points are necessary and reasonable. At least one measuring point is required.

At the location of the fault, two transient waves are propagating in both directions of the GIL. At the end of the gas insulated line a change of the characteristic impedance caused by the junction between GIL and OHL occurs. There, the waves

are partly reflected, travelling back to the fault position and are there reflected again with a reflection factor of -1 due to the short circuit (burning arc).

This process results in three clearly detectable fronts, where the second and third waveform front are dependent on the termination of the GIL.

Halving the time duration between the second and third measured front (e.g. in Figure 5 front “2b” and “3b”) and taking the propagation velocity into account, the distance of the fault from the evaluated measuring point is obtained.

At which side of the measuring point the fault position is located has to be identified individually. This can be done by analysing the recorded steep front, as demonstrated in the following examples:

- If the GIL has two different terminations e.g. transformer and OHL, the fault position can be derived by analysing the amplitude and shape of the reflected signal “2”.

- If the distance of the measuring point to both ends of the GIL is known, the fault position can be derived by analysing the time difference between the first and the second steep front.

Furthermore, it is reasonable to have more than one measuring point installed within a gas insulated transmission line:

- If the fault position is near to the measuring point it can be difficult to determine the exact fault position due to superposition of the second and third steep front.

- If a secondary breakdown occurs on the site of the internal flashover which is not equipped with measurement technique, it is not possible to detect the secondary breakdown.

6 CONCLUSION AND DISCUSSION

The propagation velocity of transient signals within a gas insulated transmission line is estimated to be 99.2 % of the speed of light.

It was not possible to measure an attenuation influence of the gas insulated transmission line after either a distance of around 530 m or after taking the complete signal decay of the test setup into account.

With the developed calculation tool taking the theoretical frequency dependent transmission characteristic of the gas insulated transmission line into account it is estimated that the signal attenuation of a lightning impulse voltage after 25 km is very small.

An attenuation influence due to the availability of disc insulators could not be observed for signals which are in the frequency range of some MHz, e.g. disconnector switching. Instead, in [7] it is shown that the disc insulators have a not negligible impact on travelling waves if the rise time is 1 ns. This effect disappears with increasing rise times acc. to the measurements in this paper. Furthermore, the disc insulators have a major attenuation impact for partial discharges which have frequencies included up to the GHz range [8].

This means that for insulation coordination studies concerning gas insulated transmission lines with lengths of a few ten kilometres the GIL could be modelled lossless and with a propagation velocity of the speed of light.

With different measuring points within the GIL it is possible to locate the fault position of an internal flashover by analysing the recorded steep fronts by oscilloscopes.

7 REFERENCES

[1] C. Neumann, I. Jürgens, J. Alter, S. Poehler: „Pilot Installation of a 380 kV Directly Buried Gas Insulated Line (GIL)”, Cigre B3_104, 2010

[2] A. Miyazaki, N. Takinami, S. Kobayashi, T. Yamauchi, H. Hama, T. Araki, H. Nishima, H. Hata, H. Yamaguchi: “Line Constant Measurements and Loading Current Test in Long-Distance 275 kV GIL”, IEEE Transactions on Power Delivery, Vol. 16, No. 2, pp. 165-170, 2001

[3] R. Weber: “Simultandurchschläge in SF_6-isolierten metallgekapselten Schaltanlagen“, VDI Fortschrittsberichte, Reihe 21, Nr. 204, Technische Universität München, 1996

[4] M. Beyer, W. Boeck, K. Möller, W. Zaengl: “Hochspannungstechnik – Theoretische und praktische Grundlagen für die Anwendung”, Springer- Verlag, 1986

[5] F. W. Grover: “Inductance Calculations – Working Formulas and Table”, D. Van Nostrad Company, 1947

[6] H.-G. Unger: “Elektromagnetische Wellen auf Leitungen“, Hüthig Buch Verlag GmbH, 4. Auflage, 1996

[7] R. Witzmann: „Schnelle transiente Spannungen in metallgekapselten SF_6-isolierten Schaltanlagen“, Fortschrittsberichte VDI, Reihe 21, Nr. 55, Technische Universität München, 1989

[8] G. Schöffner: „Teilentladungsmessungen in Hochspannungsanlagen mit N_2-SF_6-Gasgemischisolation“, Dissertation, Technische Universität München, 2002